Published in final edited form as:
Exp Neurol. 2012 August ; 236(2): 351–362. doi:10.1016/j.expneurol.2012.04.018.

Macrophage Migration Inhibitory Factor (MIF) is Essential for Inflammatory and Neuropathic Pain and Enhances Pain in Response to Stress

Jessica K. Alexander[a,c,1], **Gina M. Cox**[b], **Jin-Bin Tian**[a,2], **Alicia M. Zha**[a,c], **Ping Wei**[a,c], **Kristina A. Kigerl**[a,c], **Mahesh K. Reddy**[e], **Nilesh M. Dagia**[e], **Theis Sielecki**[f], **Michael X. Zhu**[a,2], **Abhay R. Satoskar**[d], **Dana M. McTigue**[a,c], **Caroline C. Whitacre**[b,c], and **Phillip G. Popovich**[a,c]

[a]Department of Neuroscience, The Ohio State University College of Medicine, Columbus, Ohio, USA

[b]Department of Molecular Virology, Immunology & Medical Genetics, The Ohio State University College of Medicine, Columbus, Ohio, USA

[c]Center for Brain & Spinal Cord Repair, The Ohio State University College of Medicine, Columbus, Ohio, USA

[d]Pathology, The Ohio State University College of Medicine, Columbus, Ohio, USA

[e]Piramal Life Sciences Limited, Mumbai, India

[f]Cytokine PharmaSciences Inc., King of Prussia, Pennsylvania, USA

Abstract

Stress and glucocorticoids exacerbate pain via undefined mechanisms. Macrophage migration inhibitory factor (MIF) is a constitutively expressed protein that is secreted to maintain immune function when glucocorticoids are elevated by trauma or stress. Here we show that MIF is essential for the development of neuropathic and inflammatory pain, and for stress-induced enhancement of neuropathic pain. *Mif* null mutant mice fail to develop pain-like behaviors in response to inflammatory stimuli or nerve injury. Pharmacological inhibition of MIF attenuates pain-like behaviors caused by nerve injury and prevents sensitization of these behaviors by stress. Conversely, injection of recombinant MIF into naïve mice produces dose-dependent mechanical sensitivity that is exacerbated by stress. MIF elicits pro-inflammatory signaling in microglia and activates sensory neurons, mechanisms that underlie pain. These data implicate MIF as a key regulator of pain and provide a mechanism whereby stressors exacerbate pain. MIF inhibitors warrant clinical investigation for the treatment of chronic pain.

Corresponding author: Phillip G. Popovich, The Ohio State University, 460 West 12th Avenue, 786 Biomedical Research Tower, Columbus Ohio 43210; ph: 614.688.8576; fax: 614.688.5463; Phillip.Popovich@osumc.edu.
[1]Present Address: Hospital for Sick Children, Toronto, Ontario, Canada
[2]Present Address: University of Texas Health Science Center, Houston, Texas, USA

Commercial Interests: Drs. Dagia, Reddy, and Sielecki are employees of pharmaceutical companies that provided reagents.

Keywords

MIF; Pain; Stress; Glucocorticoids; Axon; Neuroplasticity; Microglia; Macrophage; Cytokine; Inflammation

Introduction

There is an urgent need for new treatment options in the prevention and management of chronic pain. An estimated 20–30% of the world's adult population experience chronic pain (Gureje et al., 1998; Harstall, 2003). Present therapies are inadequate and poorly managed pain leads to physical and psychological disability, reduced quality of life, and significant cost burden to healthcare providers and society (Katz and Barkin, 2010; Stewart et al., 2003).

Psychological stress can exacerbate the frequency and severity of pain (Turk et al., 2010). Exactly how pain is initiated or amplified by stress is poorly understood; however, pre-clinical data indicate that endogenous glucocorticoids (GCs), the primary stress hormone, aggravate pain (Alexander et al., 2009; Khasar et al., 2008; Wang et al., 2004). GCs exert anti-inflammatory and immunosuppressive actions, which are proposed to be counterbalanced by another hormone, macrophage migration inhibitory factor (MIF). MIF is a pituitary-derived hormone secreted in tandem with GCs during stress and circadian pulsatility (Bernhagen et al., 1993; Calandra et al., 1995; Petrovsky et al., 2003). It was first described as a T cell cytokine, named for its ability to cause macrophage arrest in inflammatory exudates (Bloom and Bennett, 1966; David, 1966). MIF is now recognized as a pro-inflammatory cytokine and an endocrine hormone. Basal circulating concentrations of MIF are ~1000-fold greater than other pro-inflammatory cytokines (e.g., IL-1β, TNF-α, IL-6) (Aloisi et al., 2005; Bucala, 1996; Calandra and Roger, 2003).

Many cytokines and hormones are released during injury or inflammation, and these factors regulate neuronal encoding of painful sensations. For example, in pre-clinical models, inflammatory cytokines cause or amplify nociception by enhancing neuron excitability (Fukuoka et al., 1994; Jin and Gereau, 2006; Jung et al., 2008; Obreja et al., 2005; Oh et al., 2001; Ozaktay et al., 2006; Schafers et al., 2003a; von Banchet et al., 2005; Zhang et al., 2002). Endocrine hormones (e.g., GCs, estrogen) also regulate neuronal activity in painful states, causing heightened sensitivity or analgesia (Hucho et al., 2006; Wang et al., 2005). Whether MIF influences pain in the presence or absence of concurrent stress is largely unknown.

Here, we tested the hypotheses that MIF contributes to the development of pain and also to the sensitization of pain behaviors by stress. Our data show that MIF is required for the onset of pain caused by nerve injury or inflammation. Further, MIF alone is algogenic and acts as a downstream mediator of stress effects on pain; MIF inhibition prevents stress-induced exacerbation of pain. The robust effects of MIF can be explained by MIF acting on microglia and neurons; MIF elicits pro-inflammatory signaling in microglia and triggers functional and anatomical plasticity in sensory neurons. Together, these data implicate MIF as a key regulator of pain and enhanced pain responses caused by stress.

Materials & Methods

Animals

Adult female (8–10 weeks) MIF-null mutant (*Mif*$^{-/-}$) or wild type (WT) mice were used for most experiments. *Mif*$^{-/-}$ mice (B6;129S4-*Mif*^{tm1Dvd}) were generated as previously

described and extensively backcrossed (>10 generations) onto a C57BL/6 background (Bozza et al., 1999). Offspring were genotyped using PCR to confirm deletion of *Mif* (Fig. 1). Primers used to amplify DNA were: neo (forward, 5′-CGTCCAGATCATCCTGATC-3′; reverse, 5′-ATTGAACAAGATGGATTGCAC-3′) and *Mif* (forward, 5′-AGACCACGTGCTTAGCTGAG-3′; reverse, 5′-GCATCGCTACCGGTGGATAA-3′). C57BL/6 WT mice were obtained from Taconic (Germantown, NY) or in-house colony. Adult or early postnatal female Sprague-Dawley rats (Harlan, Houston, TX) were a source of tissue or primary microglia, respectively (see Figs. 3&4). Although most data were generated using mice, rats also were used as experimental subjects because of inherent limitations or issues of feasibility using mouse cells/tissues with select assays or reagent(s). To the extent possible, data were confirmed in both species.

Animals were group-housed in standard cages with *ad libitum* access to food and water. Animals were habituated and maintained in a vivarium with controlled temperature (~20° C) on a 12 hr light/dark cycle. Behavioral testing was performed during the light cycle by an experimenter unaware of procedure, genotype, and/or treatment. All procedures were conducted in accordance with protocols approved by the Ohio State University Institutional Laboratory Animal Care and Use Committee and with the guidelines of the Committee for Research and Ethical Issues of International Association for the Study of Pain.

Drugs

Recombinant human MIF (rMIF) was prepared as previously described (Dagia et al., 2009) (Piramal Life Sciences Limited, Mumbai, India) and delivered in sterile phosphate buffered saline (PBS) vehicle (Veh). We tested the efficacy of two small molecule MIF inhibitors (MIFi), Iso-1 (0.5–1 mg/mouse in Fig. 2B; 100 μM in 4B; Calbiochem (Gibbstown, NJ)) and CPSI-1306 (10 mg/kg; Fig. 8A; Cytokine PharmaSciences (King of Prussia, PA)). Selectivity and potency for these compounds have been described (Aroca et al., 1991; Kithcart et al., 2010; Lubetsky et al., 2002). The compounds were prepared in 10% DMSO in sterile PBS. Lipopolysaccharide (LPS; *E. coli* 055:B5) and complete Freund's adjuvant (CFA) were obtained from Sigma. Nerve growth factor (NGF) was obtained from AbD Serotec (Raleigh, NC).

Restraint stress protocol

Mice assigned to experimental groups incorporating stress were placed individually into well-ventilated polypropylene tubes (2.8 cm internal diameter, 9.7 cm length) for 60 min. Mice had no previous exposure to the tube, which permits minimal, confined movement including postural adjustments. This acute restraint stress paradigm causes circulating levels of corticosterone to increase ~300–400% with return to pre-stress levels within 2 h (Alexander et al., 2009; Flint et al., 2005; Qin and Smith, 2008). Mice not subjected to stress (No Stress groups) remained undisturbed in their home cages.

Peripheral nerve injury

The spared nerve injury (SNI) procedure was performed using aseptic technique as described previously (Alexander et al., 2009; Shields et al., 2003). This is a widely used model of neuropathic pain in which the tibial branch of the sciatic nerve is spared. In contrast to a similar model of SNI where the sural branch of the sciatic nerve is spared (Bourquin et al., 2006), the duration of peak mechanical hypersensitivity is reduced with tibial nerve sparing (Alexander et al., 2009; Shields et al., 2003). Mice were anesthetized (isoflurane anesthesia in oxygen-enriched air; 4% induction/1.5% maintenance) then an incision of the skin and biceps femoris muscle was made at the upper-thigh level to expose the sciatic nerve and its three terminal branches. Two of the branches, the sural and common peroneal nerves, were tightly ligated with 7-0 silk suture (Genzyme Biosurgery, Fall River,

MA) then transected distal to the ligature. Subsequently, 1–2 mm of each nerve was resected ~1 mm distal to the ligature. The tibial nerve was left intact. The muscle/fascia layer and skin layer were closed separately with 5-0 nylon suture (Syneture, Norwalk, CT). The same injury model was applied to rats (n=3) to create injured sciatic nerve specimens for immunostaining (Fig. 3J).

Intraplantar inflammation and rMIF

A single subcutaneous (s.c.) plantar right hind paw injection (0.02 ml) of complete Freund's adjuvant (CFA; 0.5 mg/ml suspension of heat-killed *Mycobacterium tuberculosis* in mineral oil; Sigma, St. Louis, MO, USA) was performed using a 26 g sterile needle and syringe under brief anesthesia with isoflurane in oxygen. Control mice were injected with the same volume of vehicle (mineral oil). Mice were housed on soft bedding. To assess the onset of inflammation, hind paw volume was measured.

A single subcutaneous (s.c.) plantar right hind paw injection (0.02 ml) of rMIF (1000 pg) or Veh (PBS) was performed as described above. Neither CFA nor cytokines caused foot drop or autotomy and the mice groomed normally and appeared healthy.

Behavioral Testing

Punctate mechanical sensitivity was analyzed by measuring threshold responses to calibrated von Frey monofilaments (Stoelting Co., Wood Dale, IL). Mice were placed on a mesh platform in a clear compartment (8 cm × 12 cm × 5.5 cm) that permits unrestrained exploration, locomotion, and grooming in this space. Monofilaments were applied to the mid-line of the plantar surface of each hind paw using the up-down method for threshold sensitivity (Chaplan et al., 1994). The stimulus intensity threshold represents the smallest force that repeatedly elicits withdrawal of the hind paw during 10 trials (≥ 50% response sensitivity to smallest force). Threshold values represent von Frey hair handle markings that correspond to $\log_{10}$ of (10× force in mg) (Loram et al., 2009).

Thermal sensitivity was tested using the Hargreaves' method using a Plantar Test Apparatus (UgoBasile, Comerio, Italy) as described previously (Hoschouer et al., 2010). The latency to withdraw the hind paw from the infrared radiant heat stimulus (25 W) was recorded. Both hind paws were tested for 5 trials in random order with at least two minutes rest between trials. To avoid tissue damage in non-responsive mice, the heat stimulus was removed after 30 sec. The average duration across trials was used for data analyses.

Mice were acclimated to the testing procedure for 20 min/day for 2 days prior to the start of the experiment and for 10 min (von Frey) or 40 min (Hargreaves') before each session. von Frey and Hargreaves' measurements were made on different days to avoid overstimulation of the hind paws. For mice in Fig. 2B, behavioral testing was completed on days 1 and 3 post-SNI ~2 hours after injecting MIF inhibitor.

In vitro characterization of rMIF-induced microglia activation

Primary microglia were prepared as previously described (McCarthy and de Vellis, 1980; Yang et al., 2005). Meninges were removed from the brains of postnatal (P2–4) SD rats and the cerebral cortices were minced and triturated, then digested for 15 min at 37°C in S-MEM (Invitrogen, Carlsbad, CA) with 0.1% trypsin (Sigma). Trituration was resumed after the addition of 60 μg/ml DNase I (Sigma) and 10% fetal bovine serum (FBS; Hyclone) in DMEM (Invitrogen). Dissociated cells were centrifuged for 5–7 min × 1200 rpm and then cells from 5–6 rats were seeded onto a 75 cm^2 tissue culture flask coated with 100 μg/ml poly L-lysine (PLL; Sigma). Cells were maintained in DMEM containing 10% FBS with 1% Glutamax™ (Invitrogen) and 1% Pen/Strep at 37°C in a 5% CO_2 humidified incubator for 10

days, with full media changes ~ every 3 days. Cells were rinsed and media replaced after 10 days in culture followed by a 2h equilibration period in the incubator. Then, flasks were sealed with Parafilm® and shaken (250 rpm ×s ~15 h) in an orbital shaker maintained at 37 °C, and subsequently at 300 rpm for an additional 45 min. Detached cells (consisting of microglia and oligodendrocyte progenitor cells) were collected in media then plated into 24-well tissue culture dishes for 30 min at 37 °C, during which time microglia adhere to the dish. Non-adherent cells (OPCs) were removed after 30 min. The microglia (purity > 97% as determined by CD11b flow cytometry) were maintained in DMEM containing 10% FBS with 1% Glutamax™ and Pen/Strep at 37°C in a 5% CO_2 humidified incubator for 1–3 days before use in experiments. Cells incubated at 37°C in a 5% CO_2 humidified incubator were treated with rMIF at indicated concentrations and time points. The Veh control for rMIF was sterile PBS. RNA was isolated using the Trizol method (Invitrogen) and cytokine mRNA was measured using qRT-PCR as described below. Because RNA yield from primary mouse microglia was substantially lower than from rat microglia (e.g., 100 ng/ul in mouse microglia vs. 200 ng/ul using 50% fewer rat microglia), rat microglia were used for replicate experiments of dose-response (Fig. 4A) and for evaluating the effects of MIF inhibitor (Fig. 4B). For rMIF dose-response and MIF inhibition assays (Fig. 4A, B), changes in gene expression were confirmed in three independent experiments. rMIF-induced changes in gene expression were confirmed in at least one independent experiment using primary mouse microglia and also an immortalized BV-2 microglia cell line. BV-2 cells were analyzed via flow cytometry to confirm cytokine synthesis (protein) in response to rMIF (Fig. 4D, E).

Quantitative real time-PCR (qRT-PCR)

Gene-specific primer pairs for IL-1β, TNF-α, CCL2, IL-6, and iNOS were used as described previously (Kigerl et al., 2007). Gene expression was determined using qRT-PCR and compared between rMIF and Veh groups. Primer sequence specificity was confirmed by performing BLAST analysis for similar sequences against known sequence databases. PCR reactions were carried out in triplicate using 1μL cDNA/reaction and SYBR Green master mix (Applied Biosystems, Foster City, CA, USA) in 20 μL reactions. PCR product was measured using SYBR Green fluorescence collected on an Applied Biosystems 7300 system. Melting point analyses were performed for each reaction to confirm single amplified products. ΔΔCt analysis was used to normalize gene data to 18s ribosomal RNA expression.

Flow cytometry

BV-2 cells were treated with GolgiPlug (BD Biosciences, San Jose, CA) 4 h before they were collected, washed and stained for CD11b (PacificBlue; BD Biosciences), IL-6 (PE; BD Bioscience) and CCL2 (FITC; eBioscience, San Diego, CA). Events were acquired on a FACSCanto II flow cytometer (BD Biosciences). Cells were gated based on forward vs. side scatter and CD11b expression. IL-6 and CCL2 were analyzed from the $CD11b^+$ gate using FlowJo software (TreeStar, Ashland, OR). Isotype control mAbs (BD Biosciences) matched for each fluorochrome were used for cursor placement.

In vitro dorsal root ganglia (DRG) experiments

Adult mouse DRGs were harvested as described previously (Gensel et al., 2009). After 72 h at 37°C in a 5% CO_2 humidified incubator, cells were fixed with 2% paraformaldehyde in PBS. Coverslips were rinsed with 0.1 M phosphate buffer solution (PBS) and overlaid with blocking solution for 1 h. To label neurons, coverslips were incubated with anti-chicken neurofilament heavy and light chains (NF; 1:2000; Aves Labs, Tigard, OR) overnight at 4°C. Coverslips were then rinsed in 0.1 M PBS and incubated for 1 h with AlexaFluor 546-conjugated antibody in blocking solution (1:1000; Invitrogen), then rinsed in dH_2O and mounted on slides. For Western blot, cellular protein was extracted as described below.

Measures of in vitro axon growth

Twenty-four hours after plating, mouse DRG cells were treated with rMIF (at indicated concentrations), NGF (100 ng/ml) or Veh (PBS) in Neurobasal A media supplemented with 2% B27, 1% Glutamax™, and 1% penicillin-streptomycin and maintained for an additional 48 h at 37°C in a 5% CO_2 humidified incubator. Cells were then fixed with 2% paraformaldehyde in PBS and processed for immunohistochemistry as described. Three coverslips were generated for each experimental condition. At least three independent experiments were conducted for each *in vitro* manipulation. All neurons that contained at least one neurite with a length greater than the diameter of the soma were digitized using a 10x objective. To quantify the growth of individual neurons, isolated neurons were analyzed using an automated Sholl technique. This is an unbiased method for quantifying both branching complexity and axon length *in vitro* (Gensel et al., 2010).

Western Blot

Mouse spinal cord (lumbar region), DRGs (all), cortex (unilateral), hippocampus (bilateral), and pituitary gland were harvested 5 min or 1, 3 or 24 h after the onset of restraint stress or no stress. All mice were anesthetized with ketamine/xylazine (80 mg kg^{-1}/10 mg kg^{-1}; i.p.) prior to transcardial perfusion with 30 ml 0.1 M phosphate-buffered saline (PBS, pH 7.4). Tissues were collected and homogenized in mammalian protein extraction reagent (M-PER) lysis buffer (Invitrogen) containing protease and phosphatase inhibitors (Halt Cocktails; ThermoScientific; Rockford, IL). Adult mouse DRGs (Fig. 6) were plated as described previously (Gensel et al., 2009) then lysed in M-PER lysis buffer containing protease and phosphatase inhibitors (Halt Cocktails). Protein concentrations were determined by BCA Protein Assay (ThermoScientific) and samples (10 μg/well) were separated on 10% Bis-Tris gels and transferred to a nitrocellulose membrane in a wet-transfer apparatus (Invitrogen). After protein transfer, membranes were incubated with 5% BSA (ERK) or 5% milk (MIF, β-actin) for 1 h at room temperature, then with primary antibodies (1:1000 for ERK, pERK (Cell Signaling, Beverly, MA), MIF (Invitrogen) or β-actin (Sigma)) in the same blocking solution at 4°C for at least 12 h, and finally with secondary anti-IgG antibodies (1:5000 (ERK, MIF); 1:8000 (β-actin)) in 5% BSA for 1 h at room temperature. The membrane was washed three times with PBS + 5% Tween for 10 min each between incubations. HRP activity was visualized using a chemiluminescent substrate and signal density quantified with a Kodak Image Station 4000MM Pro (Carestream Health, Inc., Rochester, NY). Because of small sample sizes, heterogeneity in group variances required that data be transformed [log(10)] for normal distribution and statistical analysis (Osborne, 2002). Data in Fig. 7B–F represent the relative increase of MIF after stress compared to control (no stress). Changes in MIF are normalized to β-actin for each replicate.

Prior to lysis, DRG cells (24 h after plating) were treated for 10 min with rMIF (1000 pg/ml) or Veh (PBS) in Neurobasal A media supplemented with 2% B27, 1% Glutamax™ and 1% penicillin-streptomycin for 10 min (Fig. 6E).

ELISA

For measurement of plasma MIF, mouse cardiac blood was collected in heparin-coated tubes prior to transcardial perfusion, as described above. Round-bottom 96-well plates (Costar, Cambridge, MA) were coated with 1 μg/ml MIF capture antibody (Abcam, Cambridge, MA) in PBS + 0.02% sodium azide. Plates were incubated overnight at 4°C, washed with PBS and blocked for 2 h at 37°C with PBS + 1% BSA. Plates were washed with PBS + 0.05 Tween and incubated with 20 μl plasma for 2 h at 37°C. After washing, plates were incubated with 1 μg/ml detection antibody (biotinylated human anti-MIF, R&D) for 1 h. After washing, bound antibodies were visualized by incubating in avidin-peroxidase for 30 min followed by ABTS substate (ThermoScientific). Samples were plated in triplicate and

compared to a serial dilution curve using rMIF (R&D). Spectrophotometric readings were performed on a microplate reader at 405 nm.

Histological analyses

For cellular localization of MIF, tissues specimens were obtained from both rats and mice. Initial experiments were carried out using mouse specimens and although clear cellular labeling was evident in sections from wild type mice (but not *Mif*$^{-/-}$ mice), it was accompanied by high background labeling (e.g., Fig 3K). The same cellular distribution of MIF was observed in rat tissue but with a higher signal:noise ratio (i.e., low background labeling). Consequently, rat tissues were used to document the distribution of MIF+ cells throughout spinal cord and peripheral nerve (Fig. 3).

Mice and rats were anesthetized with a ketamine/xylazine (80 mg kg^{-1}/10 mg kg^{-1}; i.p.) cocktail prior to transcardial perfusion with 30 ml 0.1 M phosphate-buffered saline (PBS, pH 7.4) followed by 100 ml of 4% paraformaldehyde. After perfusion, tissues were rapidly removed then post-fixed for 2 h, followed by a rinse and overnight immersion in 0.2 phosphate buffer (PB) solution. Tissues were cryoprotected in 30% sucrose in 0.2 M PB for 48 h. Spinal cords (blocked in 4 mm segments centered on the L-5 level), sciatic nerves, and L4–6 DRGs were embedded in optimal cutting temperature compound (OCT; Tissue-Tek, VWR International, West Chester, PA) then frozen at −80°C. Transverse serial sections of spinal cord and longitudinal serial sections of nerve and DRG (10 μm) were cut using a cryostat, thaw-mounted on SuperFrost Plus slides (Fisher Scientific, Houston, TX) then stored at −20°C until use. After drying at room temperature, slides were rinsed with 0.1 M phosphate buffer solution (PBS) and overlaid with blocking solution (5% bovine serum albumin and 0.1% TritonX-100 (Sigma) in 0.1 M PBS) for 1 h. To label Iba-1 and MIF, slides were incubated with rabbit anti-MIF (1:2000; Invitrogen, Gland Island, NY) or rabbit anti-Iba-1 (1:750; Wako, Richmond, VA) overnight at 4°C. Chicken anti-GFAP (1:500) and neurofilaments 150 kD and 200 kD (NF; 1:1000; Aves Labs), mouse anti-CC1 (1:1000; Abcam), NeuN (1:1000; Chemicon) and OX-42 (1:1000; Serotec, Raleigh, NC) were used as above, prior to MIF. Slides were then rinsed in 0.1 M PBS and incubated with AlexaFluor 488, 546, or 633-conjugated anti-IgG antibody for 1 h at room temperature in blocking solution (1:500–1000; Invitrogen). DAPI was used when possible as a nuclear counterstain. Slides were then rinsed in dH_2O and coverslipped with Immumount (Fisher Scientific). Numerous methods were used to validate the specificity of the MIF antibody (Burry, 2000; Saper and Sawchenko, 2003). First, tissues were stained excluding primary antibodies (no primary control). No primary controls using serum from the species in which the secondary antibody was obtained also were tested. Finally, an optimal ratio of primary:secondary antibodies was applied to tissues from *Mif*$^{-/-}$ mice. No immunostaining was detected in this control (Fig. 3L). As an index of consistency of positive labeling, MIF immunoreactivity was confirmed using MIF-specific antibodies from different commercial sources (Torrey Pines, East Orange, New Jersey; Abcam) and tissues obtained from several different experiments. Our lab has validated the specificity of all other antibodies (Almad and McTigue, 2010; Ankeny et al., 2009; Sroga et al., 2003). Representative images were collected using an Olympus Flowview 1000 confocal microscope. Analysis of mouse Iba-1 expression was conducted as previously described (Alexander et al., 2009).

Electrophysiology

Coverslips plated with mouse DRG neurons (5–10k neurons/coverslip; as described above, at 18–24 h) were centered in a perfusion chamber filled with extracellular solution (ECS) containing (in mM): 145 NaCl, 5 KCl, 1 $MgCl_2$, 2 $CaCl_2$, 10 Glucose, 10 HEPES, pH7.4. rMIF was diluted in ECS and delivered via a pressure-driven perfusion system (SmartSquirt 8, AutoMate Scientific) with the tip positioned so that the DRG neuron was within the direct

stream of perfusate. Recording pipettes were pulled from micropipette glass (A-M Systems, Inc., Carlsborg, WA) to 3–5 MΩ and filled with an intracellular solution containing (in mM): 122 K-gluconate, 9 NaCl, 1.8 $MgCl_2$, 0.9 EGTA, 9 HEPES, 14 Tris-creatinePO4, 4 MgATP, 0.3 Tirs-GTP, pH 7.2). A tight (G Ω) seal and high quality break-in was made by utilizing the ez-gSEAL pressure controller (NeoBiosystems, Inc. San Jose, CA). Whole cell recordings were accomplished using an EPC10 amplifier and the PatchMaster 2.2.0 software (HEKA Electronik, Germany). As soon as the whole cell configuration was established, fast and slow capacitances were cancelled and the holding potential (Vh) was set to −60 mV. Resting membrane potential (RMP) and spontaneous firing (SF) were recorded after switching to current clamp mode, and setting current injection to zero. Depolarization-induced firing was established by injecting a sufficient current to maintain resting membrane potential at −30 mV in current clamp mode. Data were filtered at 3 kHz and digitized at 10 kHz. All recordings were made at room temperature (22–24 °C). Only one cell per cover slip was recorded to avoid possible drug contamination of other cells.

ECS perfusion was initiated when the coverslip was set in the recording chamber. The recorded neuron was perfused continuously either by ECS or 1 ng/ml rMIF in ECS. SF or depolarizing-induced firing was recorded for 12 seconds each, before, during (1 min after initiating rMIF perfusion) and after rMIF treatment.

Data analysis

Behavioral data were analyzed using repeated measures two-way ANOVA. Post-hoc analyses were conducted using Bonferroni's test. One-way ANOVA was used to analyze data with multiple groups, and Student's *t* test was used to analyze functional neuron data, or data with only one comparison. Dunnett's post-hoc test was used to analyze normalized Western blot data. An α-level of $p < 0.05$ was used as an indication of statistical significance. Statistical analyses and graphing were performed with GraphPad Prism 5 (GraphPad Software, San Diego, CA).

Results

MIF is essential for developing neuropathic or inflammatory pain

MIF is an integral signaling intermediate between the immune and endocrine systems, and both systems regulate pain (Chapman et al., 2008). As such, the ability of MIF to affect the onset, magnitude and/or duration of pain-like behaviors was tested in wild type (WT) and MIF null ($Mif^{-/-}$) mice subjected to a spared tibial nerve injury (SNI). After SNI, WT mice consistently developed mechanical hypersensitivity. Conversely, $Mif^{-/-}$ mice did not develop hypersensitivity (Fig. 2A). These observations were confirmed in three independent experiments.

Next, we tested whether pharmacological inhibition of MIF would inhibit or reduce hypersensitivity caused by SNI. Nerve-injured WT mice were treated with a small molecule MIF inhibitor (MIFi; 1 mg/mouse) or vehicle beginning at 60 min post-SNI then again 1, 2 and 3 days later (0.5 mg/mouse/day). In two independent studies, post-injury inhibition of MIF was associated with reduced mechanical hypersensitivity for at least 14 days (latest period tested; Fig. 2B). These data, when considered together with those obtained from $Mif^{-/-}$ mice, indicate that MIF regulates the development and magnitude of neuropathic pain.

Inflammation can cause chronic pain in the absence of direct mechanical trauma to the peripheral or central nervous system. To determine if MIF contributes to the development of inflammatory pain, complete Freund's adjuvant (CFA) was injected into the plantar surface of the hind paw of WT or $Mif^{-/-}$ mice. As described previously (Abbadie et al., 2003), CFA

produced paw edema, mechanical hypersensitivity and thermal hyperalgesia in WT mice. In contrast, neither mechanical nor thermal sensitivity developed in *Mif*$^{-/-}$ mice and paw edema was significantly reduced relative to WT mice (Fig. 2C–E). The small molecule MIF inhibitor also reduced allodynia by >50% compared to Veh at 1 and 3 days (data not shown). MIFi was injected i.p. at the time of i.pl. CFA injection and once daily for 3 days post-CFA. These results were confirmed in replicate studies for the *Mif*$^{-/-}$ mice and a single experiment using the MIF inhibitor.

To determine if a focal increase in MIF is sufficient to cause hypersensitivity (without nerve injury or inflammatory stimuli), recombinant MIF (rMIF) was injected into the intact hind paw of WT mice. rMIF induced hypersensitivity to a similar extent as nerve injury or intraplantar CFA (Fig. 2F). These algogenic effects were dose-dependent (10 pg–10 ng; only the effects of 1 ng are shown).

Collectively, data in Fig. 2 indicate that MIF is necessary and sufficient for the development of neuropathic or inflammatory pain; however, it is not known if MIF is acting on cellular targets within or outside the CNS. To gain insight to MIF's potential site(s) of action, immunohistochemical analyses were completed. As shown in Fig. 3, MIF is ubiquitously distributed throughout the peripheral and central nervous systems, especially within cells located in regions involved in sensory transmission. In the spinal cord, MIF was observed in a subset of dorsal horn neurons, axons and cell bodies of astrocytes, microglia and oligodendrocytes. MIF was not detected in the myelin sheath or ventral horn neurons. In the peripheral nervous system, MIF was observed in sciatic nerve and DRG. After injury of the sciatic nerve, MIF-expressing leukocytes accumulate at the site of injury (Fig. 3J). Thus, MIF is constitutively expressed within the anatomical substrates that are important for sensory transmission and can be increased at sites of injury by inflammatory cells.

MIF elicits pro-inflammatory signaling in microglia

Microglia, the resident macrophages of the central nervous system, have been implicated as cellular effectors of pain. Although peripheral macrophages adopt a pro-inflammatory phenotype in response to MIF (Bernhagen et al., 2007; Calandra et al., 1994; Gregory et al., 2006; Mitchell et al., 2002; Onodera et al., 1997), it is not known if MIF affects pro-inflammatory cytokine production by microglia. Accordingly, we tested the ability of MIF to elicit the synthesis and release of pro-algesic cytokines and chemokines from microglia (Abbadie et al., 2003; Ramer et al., 1998; Zhang et al., 2007).

rMIF consistently increased expression of TNF-α, IL-1β, IL-6, CCL2 and iNOS mRNA in primary rat and mouse microglia and immortalized BV-2 microglia (Fig. 4A; rat data shown). To confirm the specificity and necessity of rMIF for eliciting this response, rMIF was co-administered with a small molecule MIF inhibitor (MIFi; 100 μM; 6 h) after which a subset of inflammatory genes was analyzed via real-time PCR. In each case, MIFi reduced gene expression (Fig. 4B).

The inflammatory effects of rMIF on macrophages have been attributed to endotoxin contamination in available recombinant protein preparations (Kudrin and Ray, 2008). To determine whether endotoxin was present in the rMIF samples that we used to stimulate microglia, an LAL assay was performed. Only trace amounts (0.2 EU/ml or ~17 pg/ml in 100 ng/ml rMIF; Hycult Biotechnology, The Netherlands) of endotoxin were detected. When applied to BV-2 microglia, this concentration of LPS was unable to reproduce the pro-inflammatory effects of rMIF or 100 ng/ml LPS (Fig. 4C).

For a subset of cytokines and chemokines (CCL2 and IL-6), MIF-induced changes in mRNA were confirmed at the protein level using flow cytometry (100 ng/ml for 12 h; Fig.

4D, E). Lower concentrations of MIF (10 or 30 ng/ml) had no effect on CCL2 or IL-6. Western blotting for IL-6 confirmed the flow cytometry data (not shown).

Injury to the sciatic nerve causes reproducible changes in the phenotype and morphology of microglia located in the spinal cord dorsal horn. To determine if morphological parameters of microglial activation varied between *Mif*$^{-/-}$ and WT mice after SNI, dorsal horn microglia were visualized using Iba-1 immunohistochemistry. Reactive microglia were observed within superficial dorsal horn laminae in both genotypes by 3 days post-SNI; however, genotype did not affect the magnitude of this response (Fig. 5). These data are consistent with independent reports showing that morphological indices of microglial reactivity do not predict the development or extent of behavioral hypersensitivity after nerve injury (Colburn et al., 1997; Tozaki-Saitoh et al., 2008; Tsuda et al., 2009; Tsuda et al., 2003).

MIF elicits functional and anatomical plasticity in sensory neurons

Dorsal root ganglia (DRG) are comprised of neurons that convey sensory signals from the periphery to the CNS. When DRG axons are injured, neuropathic pain develops in parallel with the onset of marked structural (e.g., sprouting) and functional plasticity in the affected neurons (Woolf and Salter, 2000). Data above (see Fig. 3) indicate that MIF is co-localized within DRG and inflammatory leukocytes that accumulate at sites of injury. To determine if MIF affects DRG neurons directly, rMIF was applied to adult mouse DRG neurons *in vitro* after which indices of structural plasticity were measured. rMIF (100–1000 pg/ml) significantly increased two measures of DRG structural plasticity, i.e., axon sprouting and overall axon length (Fig. 6A–D). The magnitude of growth was comparable to that caused by treating DRG neurons with nerve growth factor (NGF), the prototypical neurotrophic factor for sensory neurons (Fig. 6C).

In non-neuronal cells, MIF activates the extracellular signal-regulated kinase (ERK) signaling pathway (Lue et al., 2005; Mitchell et al., 1999). In neurons, ERK activation is critical for stimulating axon growth/regeneration (Zhou and Snider, 2006). As shown in Fig. 6E, rMIF enhances ERK1/2 activation in DRG neurons suggesting that in response to injury, localized increases in MIF may stimulate structural plasticity.

Small diameter DRG neurons are nociceptors that transmit pain information into the CNS. To determine how MIF affects the function of presumed nociceptive neurons, we applied whole-cell patch clamp recording techniques to mouse DRG neurons in culture. Presumed nociceptive neurons were identified based on cell size (≤ 30 μm diameter) and capacitance of less than 20 pF (mean 11.5 ± 1.3 S.E.M. pF); data were collected only from DRG neurons with these characteristics. The average resting membrane potential of recorded cells was −45 ± 1.2 mV. Of the neurons tested, ~44% (7/16) fired repetitively in the current clamp mode when maintained at −30 mV by depolarizing current injection. As shown in Fig. 6F, rMIF (3 min exposure, 1 ng/ml) increased the baseline firing frequency of these neurons ~3-fold. Non-firing neurons were unaffected by rMIF. These data indicate that MIF increases the excitability of a subset of presumed nociceptive DRG neurons.

Stress-enhanced pain behaviors are MIF-dependent

The development, persistence and severity of pain are influenced by both biological and environmental factors. Psychological stress, for example, aggravates pain and pain-related disabilities (Caceres and Burns, 1997; Hall et al., 2011). Data described above implicate MIF as a pivotal biological regulator of pain hypersensitivity. Because circulating levels of MIF are increased after stress (Calandra et al., 1995), it is plausible that the stress-pain axis is regulated by MIF.

To determine if stress increases MIF within anatomical regions that are important for processing or relaying nociception and/or stress, WT mice were subjected to acute restraint stress, then at various times, semi-quantitative changes in MIF were evaluated by Western blot. Restraint stress was used because it triggers a consistent increase in circulating GCs and potentiates neuropathic pain (Alexander et al., 2009).

Five minutes after initiating restraint stress, spinal cord MIF increased 3-fold (Fig. 7A, B). By 1, 3, and 24 h post-stress, spinal MIF levels had declined but remained elevated (non-significantly) relative to no-stress control samples. MIF also increased with a similar time course in DRGs, but the magnitude of change was greater (Fig. 7A, C). In contrast, acute stress had little effect on MIF in cerebral cortex, hippocampus or pituitary gland (Fig. 7D–F). Stress increased plasma MIF as much as 300% over baseline (20.77 ng/ml ± 3.37 S.E.M.) within 24 hours (mean range of post-stress plasma MIF = 30.35 – 82.45 ng/ml).

To test the hypothesis that exacerbation of pain by stress is MIF-dependent, loss- and gain-of-function experiments were conducted. First, to block stress-induced activity of MIF, WT mice were injected with either a pharmacological inhibitor of MIF (MIFi) or vehicle 30 minutes prior to restraint stress. After 60 min of restraint, nerve injury was induced by the SNI procedure. Consistent with our previously published data (Alexander et al., 2009), stress exacerbated mechanical hypersensitivity in vehicle-treated SNI mice (measured on days 1 and 3 post-SNI; Fig. 8A). In contrast, the stress exacerbated pain-like response was prevented in mice treated with MIFi (Fig. 8A), indicating that stress-induced pain enhancement is MIF-dependent. Consistent with the pharmacological inhibition experiments, stress does not cause or enhance hypersensitivity after SNI in the absence of MIF (*Mif*$^{-/-}$) (Fig. 8A), presumably because MIF is needed to initiate a pain-like response (see Fig. 1).

Next, WT mice were subjected to restraint stress followed immediately by an intraplantar injection of rMIF. No nerve injury was superimposed. In this experiment, injection of rMIF was intended to mimic the focal accumulation of MIF that occurs in the periphery after nerve injury (see Fig. 3J). Indeed, based on data in Figs. 1 and 5 (see above), focal injection of rMIF will activate putative nociceptors and elicit pain-like behaviors without causing trauma. Hind paw sensitivity to rMIF was measured beginning 1 h after rMIF injection. Consistent with data in Fig. 2G, rMIF alone caused mechanical hypersensitivity but this response was significantly increased by prior stress (vs. no stress; Fig. 8B).

Discussion

We hypothesized that MIF, an injury- and stress-inducible cytokine and hormone, would contribute to persistent pain caused by inflammation or nerve damage. Here, we show that MIF is necessary for the development of pain hypersensitivity. Mice lacking MIF do not develop hypersensitivity after intraplantar CFA or nerve injury, and pharmacological inhibition of MIF in wild type mice suppresses hypersensitivity elicited by these stimuli. MIF is also sufficient to elicit pain-like behavior. Injection of rMIF into the hind paw of mice causes mechanical hypersensitivity that lasts for several hours. These data independently verify those reported in recent publications (Wang et al., 2010; Wang et al., 2011b) using different pain models applied to animals of different sex or species. Collectively, our data with Wang et al. demonstrate that MIF is an important determinant of pain hypersensitivity in rats and mice, in males and females, and in multiple models of inflammatory (e.g., CFA and formalin) and neuropathic pain (nerve transection and constriction).

Here, we also present novel data showing that stress effects on pain are dependent on MIF. The unexpected action of GCs, that are typically anti-inflammatory and immunosuppressive, to induce MIF (Calandra et al., 1995) suggests that MIF may underlie stress effects ascribed to GCs. Stress or elevated GCs prior to nerve injury exacerbate pain hypersensitivity (Alexander et al., 2009), therefore we predicted that stress effects on pain hypersensitivity would be influenced by MIF. We show that stress causes MIF to increase in plasma, DRG and spinal cord. Injection of a MIF inhibitor prior to stress prevents the effect of stress on nerve injury induced hypersensitivity. Thus, MIF is a potential target for therapeutic modulation of persistent pain or stress-related pain exacerbations. Based on its constitutive expression and widespread distribution throughout the central and peripheral nervous systems, MIF is poised to influence pain pathophysiology in a cell- and context- (e.g., stress) dependent manner. Data presented in this report indicate a role for MIF in regulating the function of sensory neurons and microglia, i.e., cells that play a pivotal role in regulating the onset, maintenance and severity of pain. However, the mechanism by which MIF influences pain, whether caused by inflammation or trauma, is still not clear. Techniques (e.g., transgenic and conditional knockout mice) are being developed to reveal mechanisms of action and the cell-specific role of MIF in chronic pain.

MIF could indirectly cause pain by stimulating microglia and/or macrophages to release cytokines (or other proteins) that enhance neuron excitability (Fukuoka et al., 1994; Oh et al., 2001; Ozaktay et al., 2006; Schafers et al., 2003b). Macrophages can release inflammatory mediators in response to MIF (Calandra et al., 1994; Dagia et al., 2009; Mitchell et al., 2002). In microglia, rMIF increases production of prostaglandin E2 (Wang et al., 2011a). In this report, we extend already published data by showing that MIF causes microglia to increase expression of TNF-α, IL-1β, IL-6, CCL2 and iNOS, and the effects of MIF can be blocked with a small-molecule MIF inhibitor. These inflammatory mediators are known to regulate the onset and/or severity of neuropathic pain. Interestingly, many intracellular signaling pathways (e.g., ERK, p38, Src, Jab-1, PI3K) and transcription factors (e.g., AP-1, NF-κB, NURR1, and STAT3) triggered by MIF binding to CD74, CXCR2 and/or CXCR4 on microglia and macrophages also regulate neuropathic pain states (Bernhagen et al., 2007; Crown et al., 2008; Jin et al., 2003; Mitchell et al., 1999; Onodera et al., 2004; Roger et al., 2001; Stojanovic et al., 2009; Tsuda et al., 2003; Zernecke et al., 2008; Zhuang et al., 2005). Thus, MIF likely represents an important upstream mediator of the neuroinflammatory cascades that cause or contribute to pain. MIF may also act as a paracrine or autocrine regulator of neuron function. MIF is present in sensory neurons and axons (Fig. 3), and neurons express putative MIF receptors (e.g., CD74, CXCR2 and CXCR4) (Bryan et al., 2008; Meucci et al., 1998). Novel data presented here indicate that MIF dramatically affects the structure and function of DRG neurons *in vitro*, likely via ERK activation (Fig. 6). The MIF-induced neuritogenesis in cultured DRG neurons is reminiscent of the increase in sensory afferent sprouting that occurs after nervous system injury. This form of anatomical plasticity has been implicated in the onset of neuropathic pain and spasticity (Deumens et al., 2008; Devor and Wall, 1976; McLachlan and Hu, 1998). In our studies, not only did MIF enhance structural plasticity in DRG neurons, it increased the firing rate of presumed nociceptive neurons (Fig. 6F). Accordingly, the behavioral hypersensitivity that was induced by subcutaneous injection of rMIF could be explained by local activation of nociceptors (rather than microglia or macrophages).

The circadian rhythm of MIF mirrors that of GCs (Petrovsky et al., 2003) and non-circadian triggers of GC synthesis (e.g., stress, injury, disease) also increase MIF in the circulation (Calandra et al., 1995). Since GCs and MIF have opposing effects on immune function, their concurrent regulation has been proposed as a mechanism to maintain immune homeostasis (Calandra et al., 1995). The effects of these hormones on neuronal structure and function are less clear. Although we show that sensory neurons are highly responsive to MIF, it is not

clear why tissue concentrations of MIF increase preferentially in DRGs and spinal cord, despite rising levels of MIF in plasma. Perhaps MIF and GC signaling mechanisms are enhanced in DRG and spinal cord relative to other sites in the body in order to protect the organism from potentially dangerous and painful sensory stimuli. Indeed, preliminary data from our lab indicate that GC receptors are markedly increased in DRG neurons relative to other areas of the nervous system (unpublished data). In light of the sensitivity of nociceptors to rMIF and MIF-dependent stress effects on pain, further investigation is needed to understand the mechanisms that regulate the recruitment of MIF-expressing cells, sequestration of plasma MIF, or storage of MIF mRNA in these particular regions in response to nerve injury and stress.

In summary, our results show that MIF is required for the development of persistent pain behaviors and the enhancement of pain responses by stress. As such, MIF represents a novel therapeutic target for analgesic drug development. In addition, because stress affects the severity of most health conditions, including cancer, HIV, cardiac and autoimmune diseases, the consideration of MIF as a stress-related therapeutic target could extend beyond chronic pain. The basis for the prominence of this cytokine/hormone in pain regulation requires further research. It is a highly unusual cytokine, having enzyme functions, a circadian rhythm, broad and constitutive expression, and that it is inducible by GCs (Flaster et al., 2007). The largely unexplored endocrine nature of this pro-inflammatory cytokine is likely to contribute to its role in pain. High basal expression and circulating levels underscore the importance of this cytokine, and its fluctuations, for instance during stress or circadian regulation, could produce physiological manifestations highly relevant to clinical pain presentation.

Acknowledgments

The authors thank Dr. Akshata Almad and Rezan Sahinkaya for providing rat microglia, Dr. Dustin Donnelly for IL-6 Western blot, Dr. Ming Wang for conducting nerve procedures and DRG isolations and Todd Shawler for flow cytometry assistance. This work was supported in part by NIH R01 NS047175, NS37846, and the Ray W. Poppleton Endowment (P.G.P), NIH R01 GMK081658 (P.G.P. and M.X.Z), NIH R01 NS059776 (D.M.M.), NIH AI 064320 (C.C.W.) and P30-NS045758, NIH AI 076309, AI 068829, AI 090803 (A.R.S). J.K.A. and P.G.P. formulated the hypotheses, designed the experiments and prepared the manuscript; J.K.A. conducted most experiments; G.M.C. and J.K.A. designed and conducted microglia experiments; J.B.T. and M.X.Z. designed and executed the electrophysiology studies; A.Z. assisted with neuron experiments (Fig. 5); K.A.K. helped design and complete endotoxin control experiments; M.K.R & N.M.D. prepared/provided rMIF; T.S. prepared MIF inhibitor; P.G.P., A.R.S., D.M.M. and C.C.W. supervised and supported the project.

Abbreviations

MIF	macrophage migration inhibitory factor
GCs	glucocorticoids
WT	wild type
CFA	complete Freund’s adjuvant
DRG	dorsal root ganglion

References

1. Abbadie C, Lindia JA, Cumiskey AM, Peterson LB, Mudgett JS, Bayne EK, DeMartino JA, MacIntyre DE, Forrest MJ. Impaired neuropathic pain responses in mice lacking the chemokine receptor CCR2. Proc Natl Acad Sci U S A. 2003; 100:7947–7952. [PubMed: 12808141]

2. Alexander JK, DeVries AC, Kigerl KA, Dahlman JM, Popovich PG. Stress exacerbates neuropathic pain via glucocorticoid and NMDA receptor activation. Brain Behav Immun. 2009; 23:851–860. [PubMed: 19361551]
3. Almad A, McTigue DM. Chronic expression of PPAR-delta by oligodendrocyte lineage cells in the injured rat spinal cord. J Comp Neurol. 2010; 518:785–799. [PubMed: 20058304]
4. Aloisi AM, Pari G, Ceccarelli I, Vecchi I, Ietta F, Lodi L, Paulesu L. Gender-related effects of chronic non-malignant pain and opioid therapy on plasma levels of macrophage migration inhibitory factor (MIF). Pain. 2005; 115:142–151. [PubMed: 15836977]
5. Ankeny DP, Guan Z, Popovich PG. B cells produce pathogenic antibodies and impair recovery after spinal cord injury in mice. J Clin Invest. 2009; 119:2990–2999. [PubMed: 19770513]
6. Aroca P, Solano F, Garcia-Borron JC, Lozano JA. Specificity of dopachrome tautomerase and inhibition by carboxylated indoles. Considerations on the enzyme active site. Biochem J. 1991; 277 (Pt 2):393–397. [PubMed: 1859367]
7. Bernhagen J, Calandra T, Mitchell RA, Martin SB, Tracey KJ, Voelter W, Manogue KR, Cerami A, Bucala R. MIF is a pituitary-derived cytokine that potentiates lethal endotoxaemia. Nature. 1993; 365:756–759. [PubMed: 8413654]
8. Bernhagen J, Krohn R, Lue H, Gregory JL, Zernecke A, Koenen RR, Dewor M, Georgiev I, Schober A, Leng L, Kooistra T, Fingerle-Rowson G, Ghezzi P, Kleemann R, McColl SR, Bucala R, Hickey MJ, Weber C. MIF is a noncognate ligand of CXC chemokine receptors in inflammatory and atherogenic cell recruitment. Nat Med. 2007; 13:587–596. [PubMed: 17435771]
9. Bloom BR, Bennett B. Mechanism of a reaction in vitro associated with delayed-type hypersensitivity. Science. 1966; 153:80–82. [PubMed: 5938421]
10. Bourquin AF, Suveges M, Pertin M, Gilliard N, Sardy S, Davison AC, Spahn DR, Decosterd I. Assessment and analysis of mechanical allodynia-like behavior induced by spared nerve injury (SNI) in the mouse. Pain. 2006
11. Bozza M, Satoskar AR, Lin G, Lu B, Humbles AA, Gerard C, David JR. Targeted disruption of migration inhibitory factor gene reveals its critical role in sepsis. J Exp Med. 1999; 189:341–346. [PubMed: 9892616]
12. Bryan KJ, Zhu X, Harris PL, Perry G, Castellani RJ, Smith MA, Casadesus G. Expression of CD74 is increased in neurofibrillary tangles in Alzheimer's disease. Mol Neurodegener. 2008; 3:13. [PubMed: 18786268]
13. Bucala R. MIF re-discovered: pituitary hormone and glucocorticoid-induced regulator of cytokine production. Cytokine Growth Factor Rev. 1996; 7:19–24. [PubMed: 8864351]
14. Burry RW. Specificity controls for immunocytochemical methods. J Histochem Cytochem. 2000; 48:163–166. [PubMed: 10639482]
15. Caceres C, Burns JW. Cardiovascular reactivity to psychological stress may enhance subsequent pain sensitivity. Pain. 1997; 69:237–244. [PubMed: 9085297]
16. Calandra T, Bernhagen J, Metz CN, Spiegel LA, Bacher M, Donnelly T, Cerami A, Bucala R. MIF as a glucocorticoid-induced modulator of cytokine production. Nature. 1995; 377:68–71. [PubMed: 7659164]
17. Calandra T, Bernhagen J, Mitchell RA, Bucala R. The macrophage is an important and previously unrecognized source of macrophage migration inhibitory factor. J Exp Med. 1994; 179:1895–1902. [PubMed: 8195715]
18. Calandra T, Roger T. Macrophage migration inhibitory factor: a regulator of innate immunity. Nat Rev Immunol. 2003; 3:791–800. [PubMed: 14502271]
19. Chaplan SR, Bach FW, Pogrel JW, Chung JM, Yaksh TL. Quantitative assessment of tactile allodynia in the rat paw. J Neurosci Methods. 1994; 53:55–63. [PubMed: 7990513]
20. Chapman CR, Tuckett RP, Song CW. Pain and stress in a systems perspective: reciprocal neural, endocrine, and immune interactions. J Pain. 2008; 9:122–145. [PubMed: 18088561]
21. Colburn RW, DeLeo JA, Rickman AJ, Yeager MP, Kwon P, Hickey WF. Dissociation of microglial activation and neuropathic pain behaviors following peripheral nerve injury in the rat. J Neuroimmunol. 1997; 79:163–175. [PubMed: 9394789]

22. Crown ED, Gwak YS, Ye Z, Johnson KM, Hulsebosch CE. Activation of p38 MAP kinase is involved in central neuropathic pain following spinal cord injury. Exp Neurol. 2008; 213:257–267. [PubMed: 18590729]
23. Dagia NM, Kamath DV, Bhatt P, Gupte RD, Dadarkar SS, Fonseca L, Agarwal G, Chetrapal-Kunwar A, Balachandran S, Srinivasan S, Bose J, Pari K, CBR, Parkale SS, Gadekar PK, Rodge AH, Mandrekar N, Vishwakarma RA, Sharma S. A fluorinated analog of ISO-1 blocks the recognition and biological function of MIF and is orally efficacious in a murine model of colitis. Eur J Pharmacol. 2009; 607:201–212. [PubMed: 19239912]
24. David JR. Delayed hypersensitivity in vitro: its mediation by cell-free substances formed by lymphoid cell-antigen interaction. Proc Natl Acad Sci U S A. 1966; 56:72–77. [PubMed: 5229858]
25. Deumens R, Joosten EA, Waxman SG, Hains BC. Locomotor dysfunction and pain: the scylla and charybdis of fiber sprouting after spinal cord injury. Mol Neurobiol. 2008; 37:52–63. [PubMed: 18415034]
26. Devor M, Wall PD. Type of sensory nerve fibre sprouting to form a neuroma. Nature. 1976; 262:705–708. [PubMed: 958442]
27. Flaster H, Bernhagen J, Calandra T, Bucala R. The macrophage migration inhibitory factor-glucocorticoid dyad: regulation of inflammation and immunity. Mol Endocrinol. 2007; 21:1267–1280. [PubMed: 17389748]
28. Flint MS, Carroll JE, Jenkins FJ, Chambers WH, Han ML, Baum A. Genomic profiling of restraint stress-induced alterations in mouse T lymphocytes. J Neuroimmunol. 2005; 167:34–44. [PubMed: 16026860]
29. Fukuoka H, Kawatani M, Hisamitsu T, Takeshige C. Cutaneous hyperalgesia induced by peripheral injection of interleukin-1 beta in the rat. Brain Res. 1994; 657:133–140. [PubMed: 7820610]
30. Gensel JC, Nakamura S, Guan Z, van Rooijen N, Ankeny DP, Popovich PG. Macrophages promote axon regeneration with concurrent neurotoxicity. J Neurosci. 2009; 29:3956–3968. [PubMed: 19321792]
31. Gensel JC, Schonberg DL, Alexander JK, McTigue DM, Popovich PG. Semi-automated Sholl analysis for quantifying changes in growth and differentiation of neurons and glia. J Neurosci Methods. 2010; 190:71–79. [PubMed: 20438758]
32. Gregory JL, Morand EF, McKeown SJ, Ralph JA, Hall P, Yang YH, McColl SR, Hickey MJ. Macrophage migration inhibitory factor induces macrophage recruitment via CC chemokine ligand 2. J Immunol. 2006; 177:8072–8079. [PubMed: 17114481]
33. Gureje O, Von Korff M, Simon GE, Gater R. Persistent pain and well-being: a World Health Organization Study in Primary Care. JAMA. 1998; 280:147–151. [PubMed: 9669787]
34. Hall AM, Kamper SJ, Maher CG, Latimer J, Ferreira ML, Nicholas MK. Symptoms of depression and stress mediate the effect of pain on disability. Pain. 2011; 152:1044–1051. [PubMed: 21306826]
35. Harstall, C. How Prevalent is Chronic Pain?. In: Carr, D., editor. PAIN Clinical Updates. International Association for the Study of Pain; Seattle: 2003.
36. Hoschouer EL, Basso DM, Jakeman LB. Aberrant sensory responses are dependent on lesion severity after spinal cord contusion injury in mice. Pain. 2010; 148:328–342. [PubMed: 20022699]
37. Hucho TB, Dina OA, Kuhn J, Levine JD. Estrogen controls PKCepsilon-dependent mechanical hyperalgesia through direct action on nociceptive neurons. Eur J Neurosci. 2006; 24:527–534. [PubMed: 16836642]
38. Jin SX, Zhuang ZY, Woolf CJ, Ji RR. p38 mitogen-activated protein kinase is activated after a spinal nerve ligation in spinal cord microglia and dorsal root ganglion neurons and contributes to the generation of neuropathic pain. J Neurosci. 2003; 23:4017–4022. [PubMed: 12764087]
39. Jin X, Gereau RW IV. Acute p38-Mediated Modulation of Tetrodotoxin-Resistant Sodium Channels in Mouse Sensory Neurons by Tumor Necrosis Factor-{alpha}. J Neurosci. 2006; 26:246–255. [PubMed: 16399694]
40. Jung H, Toth PT, White FA, Miller RJ. Monocyte chemoattractant protein-1 functions as a neuromodulator in dorsal root ganglia neurons. J Neurochem. 2008; 104:254–263. [PubMed: 17944871]

41. Katz WA, Barkin RL. Dilemmas in chronic/persistent pain management. Dis Mon. 2010; 56:233–250. [PubMed: 20350655]
42. Khasar SG, Burkham J, Dina OA, Brown AS, Bogen O, Alessandri-Haber N, Green PG, Reichling DB, Levine JD. Stress induces a switch of intracellular signaling in sensory neurons in a model of generalized pain. J Neurosci. 2008; 28:5721–5730. [PubMed: 18509033]
43. Kigerl KA, Lai W, Rivest S, Hart RP, Satoskar AR, Popovich PG. Toll-like receptor (TLR)-2 and TLR-4 regulate inflammation, gliosis, and myelin sparing after spinal cord injury. J Neurochem. 2007; 102:37–50. [PubMed: 17403033]
44. Kithcart AP, Cox GM, Sielecki T, Short A, Pruitt J, Papenfuss T, Shawler T, Gienapp I, Satoskar AR, Whitacre CC. A small-molecule inhibitor of macrophage migration inhibitory factor for the treatment of inflammatory disease. FASEB J. 2010; 24:4459–4466. [PubMed: 20624927]
45. Kudrin A, Ray D. Cunning factor: macrophage migration inhibitory factor as a redox-regulated target. Immunol Cell Biol. 2008; 86:232–238. [PubMed: 18040285]
46. Loram LC, Harrison JA, Sloane EM, Hutchinson MR, Sholar P, Taylor FR, Berkelhammer D, Coats BD, Poole S, Milligan ED, Maier SF, Rieger J, Watkins LR. Enduring reversal of neuropathic pain by a single intrathecal injection of adenosine 2A receptor agonists: a novel therapy for neuropathic pain. J Neurosci. 2009; 29:14015–14025. [PubMed: 19890011]
47. Lubetsky JB, Dios A, Han J, Aljabari B, Ruzsicska B, Mitchell R, Lolis E, Al-Abed Y. The tautomerase active site of macrophage migration inhibitory factor is a potential target for discovery of novel anti-inflammatory agents. J Biol Chem. 2002; 277:24976–24982. [PubMed: 11997397]
48. Lue H, Kapurniotu A, Fingerle-Rowson G, Roger T, Leng L, Thiele M, Calandra T, Bucala R, Bernhagen J. Rapid and transient activation of the ERK MAPK signalling pathway by macrophage migration inhibitory factor (MIF) and dependence on JAB1/CSN5 and Src kinase activity. Cell Signal. 2005
49. McCarthy KD, de Vellis J. Preparation of separate astroglial and oligodendroglial cell cultures from rat cerebral tissue. J Cell Biol. 1980; 85:890–902. [PubMed: 6248568]
50. McLachlan EM, Hu P. Axonal sprouts containing calcitonin gene-related peptide and substance P form pericellular baskets around large diameter neurons after sciatic nerve transection in the rat. Neuroscience. 1998; 84:961–965. [PubMed: 9578389]
51. Meucci O, Fatatis A, Simen AA, Bushell TJ, Gray PW, Miller RJ. Chemokines regulate hippocampal neuronal signaling and gp120 neurotoxicity. Proc Natl Acad Sci U S A. 1998; 95:14500–14505. [PubMed: 9826729]
52. Mitchell RA, Liao H, Chesney J, Fingerle-Rowson G, Baugh J, David J, Bucala R. Macrophage migration inhibitory factor (MIF) sustains macrophage proinflammatory function by inhibiting p53: regulatory role in the innate immune response. Proc Natl Acad Sci U S A. 2002; 99:345–350. [PubMed: 11756671]
53. Mitchell RA, Metz CN, Peng T, Bucala R. Sustained mitogen-activated protein kinase (MAPK) and cytoplasmic phospholipase A2 activation by macrophage migration inhibitory factor (MIF). Regulatory role in cell proliferation and glucocorticoid action. J Biol Chem. 1999; 274:18100–18106. [PubMed: 10364264]
54. Obreja O, Biasio W, Andratsch M, Lips KS, Rathee PK, Ludwig A, Rose-John S, Kress M. Fast modulation of heat-activated ionic current by proinflammatory interleukin 6 in rat sensory neurons. Brain. 2005; 128:1634–1641. [PubMed: 15817518]
55. Oh SB, Tran PB, Gillard SE, Hurley RW, Hammond DL, Miller RJ. Chemokines and glycoprotein120 produce pain hypersensitivity by directly exciting primary nociceptive neurons. J Neurosci. 2001; 21:5027–5035. [PubMed: 11438578]
56. Onodera S, Nishihira J, Koyama Y, Majima T, Aoki Y, Ichiyama H, Ishibashi T, Minami A. Macrophage migration inhibitory factor up-regulates the expression of interleukin-8 messenger RNA in synovial fibroblasts of rheumatoid arthritis patients: common transcriptional regulatory mechanism between interleukin-8 and interleukin-1beta. Arthritis Rheum. 2004; 50:1437–1447. [PubMed: 15146413]

57. Onodera S, Suzuki K, Matsuno T, Kaneda K, Takagi M, Nishihira J. Macrophage migration inhibitory factor induces phagocytosis of foreign particles by macrophages in autocrine and paracrine fashion. Immunology. 1997; 92:131–137. [PubMed: 9370935]
58. Osborne J. Notes on the use of data transformations. Practical Assessment, Research & Evaluation. 2002; 8
59. Ozaktay AC, Kallakuri S, Takebayashi T, Cavanaugh JM, Asik I, DeLeo JA, Weinstein JN. Effects of interleukin-1 beta, interleukin-6, and tumor necrosis factor on sensitivity of dorsal root ganglion and peripheral receptive fields in rats. Eur Spine J. 2006; 15:1529–1537. [PubMed: 16474945]
60. Petrovsky N, Socha L, Silva D, Grossman AB, Metz C, Bucala R. Macrophage migration inhibitory factor exhibits a pronounced circadian rhythm relevant to its role as a glucocorticoid counter-regulator. Immunol Cell Biol. 2003; 81:137–143. [PubMed: 12631237]
61. Qin M, Smith CB. Unaltered hormonal response to stress in a mouse model of fragile X syndrome. Psychoneuroendocrinology. 2008; 33:883–889. [PubMed: 18479837]
62. Ramer MS, Murphy PG, Richardson PM, Bisby MA. Spinal nerve lesion-induced mechanoallodynia and adrenergic sprouting in sensory ganglia are attenuated in interleukin-6 knockout mice. Pain. 1998; 78:115–121. [PubMed: 9839821]
63. Roger T, David J, Glauser MP, Calandra T. MIF regulates innate immune responses through modulation of Toll-like receptor 4. Nature. 2001; 414:920–924. [PubMed: 11780066]
64. Saper CB, Sawchenko PE. Magic peptides, magic antibodies: guidelines for appropriate controls for immunohistochemistry. J Comp Neurol. 2003; 465:161–163. [PubMed: 12949777]
65. Schafers M, Lee DH, Brors D, Yaksh TL, Sorkin LS. Increased Sensitivity of Injured and Adjacent Uninjured Rat Primary Sensory Neurons to Exogenous Tumor Necrosis Factor-alpha after Spinal Nerve Ligation. J Neurosci. 2003a; 23:3028–3038. [PubMed: 12684490]
66. Schafers M, Svensson CI, Sommer C, Sorkin LS. Tumor Necrosis Factor-alpha Induces Mechanical Allodynia after Spinal Nerve Ligation by Activation of p38 MAPK in Primary Sensory Neurons. J Neurosci. 2003b; 23:2517–2521. [PubMed: 12684435]
67. Shields SD, Eckert WA 3rd, Basbaum AI. Spared nerve injury model of neuropathic pain in the mouse: a behavioral and anatomic analysis. J Pain. 2003; 4:465–470. [PubMed: 14622667]
68. Sroga JM, Jones TB, Kigerl KA, McGaughy VM, Popovich PG. Rats and mice exhibit distinct inflammatory reactions after spinal cord injury. J Comp Neurol. 2003; 462:223–240. [PubMed: 12794745]
69. Stewart WF, Ricci JA, Chee E, Morganstein D, Lipton R. Lost productive time and cost due to common pain conditions in the US workforce. JAMA. 2003; 290:2443–2454. [PubMed: 14612481]
70. Stojanovic I, Cvjeticanin T, Lazaroski S, Stosic-Grujicic S, Miljkovic D. Macrophage migration inhibitory factor stimulates interleukin-17 expression and production in lymph node cells. Immunology. 2009; 126:74–83. [PubMed: 18624729]
71. Tozaki-Saitoh H, Tsuda M, Miyata H, Ueda K, Kohsaka S, Inoue K. P2Y12 receptors in spinal microglia are required for neuropathic pain after peripheral nerve injury. J Neurosci. 2008; 28:4949–4956. [PubMed: 18463248]
72. Tsuda M, Masuda T, Kitano J, Shimoyama H, Tozaki-Saitoh H, Inoue K. IFN-gamma receptor signaling mediates spinal microglia activation driving neuropathic pain. Proc Natl Acad Sci U S A. 2009; 106:8032–8037. [PubMed: 19380717]
73. Tsuda M, Shigemoto-Mogami Y, Koizumi S, Mizokoshi A, Kohsaka S, Salter MW, Inoue K. P2X4 receptors induced in spinal microglia gate tactile allodynia after nerve injury. Nature. 2003; 424:778–783. [PubMed: 12917686]
74. Turk DC, Audette J, Levy RM, Mackey SC, Stanos S. Assessment and treatment of psychosocial comorbidities in patients with neuropathic pain. Mayo Clin Proc. 2010; 85:S42–50. [PubMed: 20194148]
75. von Banchet GS, Kiehl M, Schaible HG. Acute and long-term effects of IL-6 on cultured dorsal root ganglion neurones from adult rat. J Neurochem. 2005; 94:238–248. [PubMed: 15953366]
76. Wang F, Shen X, Guo X, Peng Y, Liu Y, Xu S, Yang J. Spinal macrophage migration inhibitory factor contributes to the pathogenesis of inflammatory hyperalgesia in rats. Pain. 2010; 148:275–283. [PubMed: 20005040]

77. Wang F, Wu H, Xu S, Guo X, Yang J, Shen X. Macrophage migration inhibitory factor activates cyclooxygenase 2-prostaglandin E(2) in cultured spinal microglia. Neurosci Res. 2011a; 71:210–218. [PubMed: 21802455]

78. Wang F, Xu S, Shen X, Guo X, Peng Y, Yang J. Spinal macrophage migration inhibitory factor is a major contributor to rodent neuropathic pain-like hypersensitivity. Anesthesiology. 2011b; 114:643–659. [PubMed: 21293254]

79. Wang S, Lim G, Zeng Q, Sung B, Ai Y, Guo G, Yang L, Mao J. Expression of central glucocorticoid receptors after peripheral nerve injury contributes to neuropathic pain behaviors in rats. J Neurosci. 2004; 24:8595–8605. [PubMed: 15456833]

80. Wang S, Lim G, Zeng Q, Sung B, Yang L, Mao J. Central glucocorticoid receptors modulate the expression and function of spinal NMDA receptors after peripheral nerve injury. J Neurosci. 2005; 25:488–495. [PubMed: 15647493]

81. Woolf CJ, Salter MW. Neuronal plasticity: increasing the gain in pain. Science. 2000; 288:1765–1769. [PubMed: 10846153]

82. Yang Z, Watanabe M, Nishiyama A. Optimization of oligodendrocyte progenitor cell culture method for enhanced survival. J Neurosci Methods. 2005; 149:50–56. [PubMed: 15975663]

83. Zernecke A, Bernhagen J, Weber C. Macrophage migration inhibitory factor in cardiovascular disease. Circulation. 2008; 117:1594–1602. [PubMed: 18362243]

84. Zhang J, Shi XQ, Echeverry S, Mogil JS, De Koninck Y, Rivest S. Expression of CCR2 in both resident and bone marrow-derived microglia plays a critical role in neuropathic pain. J Neurosci. 2007; 27:12396–12406. [PubMed: 17989304]

85. Zhang JM, Li H, Liu B, Brull SJ. Acute topical application of tumor necrosis factor alpha evokes protein kinase A-dependent responses in rat sensory neurons. J Neurophysiol. 2002; 88:1387–1392. [PubMed: 12205159]

86. Zhou FQ, Snider WD. Intracellular control of developmental and regenerative axon growth. Philos Trans R Soc Lond B Biol Sci. 2006; 361:1575–1592. [PubMed: 16939976]

87. Zhuang ZY, Gerner P, Woolf CJ, Ji RR. ERK is sequentially activated in neurons, microglia, and astrocytes by spinal nerve ligation and contributes to mechanical allodynia in this neuropathic pain model. Pain. 2005; 114:149–159. [PubMed: 15733640]

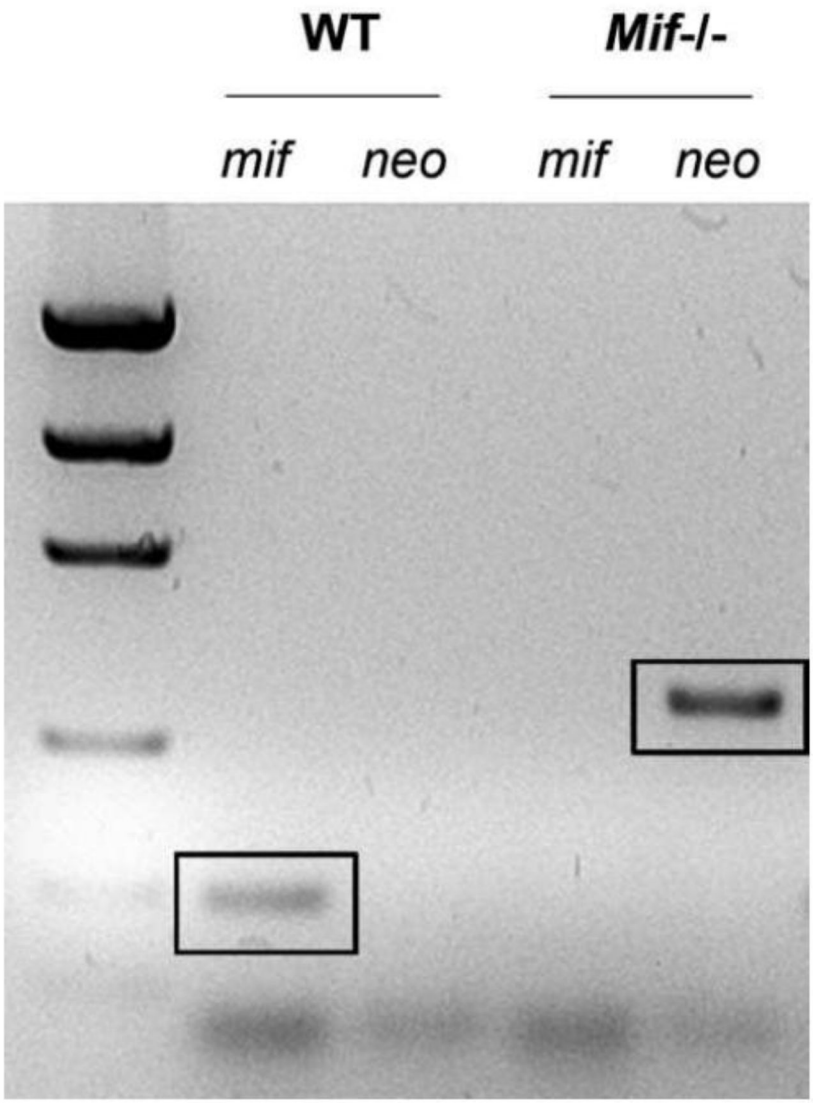

Figure 1.
All offspring from a colony of *Mif*−/− mice were genotyped via PCR to confirm deletion of *Mif*. The presence of the neo cassette indicates gene deletion (representative screen from a *Mif*−/− mouse generated at OSU). See Methods for primers used to amplify *Mif* and neo cassette.

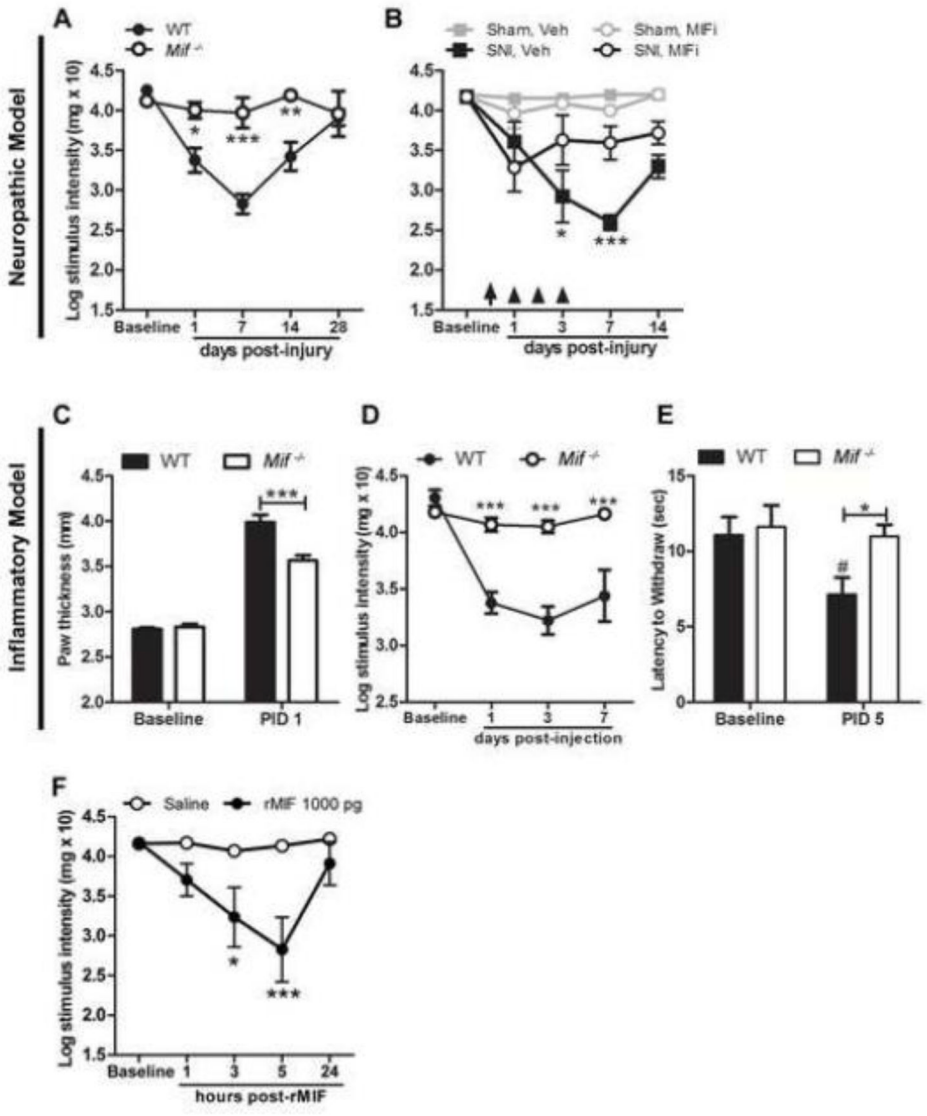

Figure 2.

MIF regulates the onset and magnitude of neuropathic or inflammatory pain-like behaviors. ***A***, Unlike wild type (WT) mice, *Mif*−/− mice do not develop mechanical hypersensitivity after nerve injury. ***B***, Systemic injection of a MIF inhibitor (MIFi) after nerve injury reduces hypersensitivity (treatments indicated by arrow (60 min post-SNI) and arrowheads (days 1–3 post-SNI)). ***C***, Edema caused by i.pl. CFA is reduced in *Mif*−/− mice at post-injection day (PID) 1. ***D***, CFA induces mechanical hypersensitivity and ***E***, thermal hyperalgesia in WT mice but not *Mif*−/− mice. ***F***, Intraplantar injection of rMIF (1000 pg) produces mechanical hypersensitivity. *A, B, D, F*: y-axis values represent von Frey hair handle markings where 4.31=2 grams of force and 2.83=0.07 grams of force. N=5/group. Results are expressed as mean ± SEM. Statistical comparisons are between *Mif*−/− and WT mice (A, C, D, E), or SNI, Veh and SNI, MIFi (B) or Saline and rMIF (F) groups., $*p<0.05$; $**p<0.01$; $***p<0.0001$. In *E*, # denotes $p<0.05$ when comparing WT Baseline vs. PID 5.

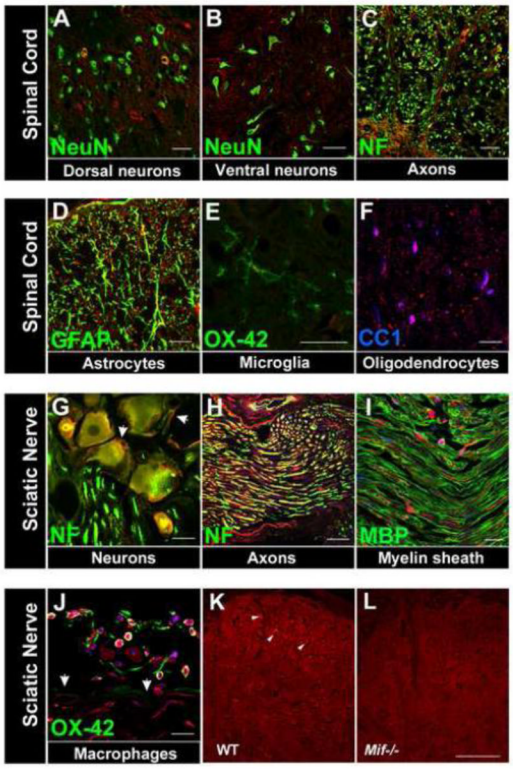

Figure 3.

MIF is constitutively expressed in the rat spinal cord (A–F) and rat peripheral nervous system (G–I). Superimposed confocal images showing MIF (red) and cell-specific markers (green or blue). ***A,B*** MIF is expressed in a subset of spinal cord dorsal horn ***(A)*** neurons (green; NeuN) but not ventral horn motor neurons ***(B)***. ***C–F***, MIF is also expressed in spinal cord axons (***C***, green: neurofilament (NF), astrocytes (***D***, green: GFAP), microglia (***E***, green: OX-42) and oligodendrocytes (***F***, blue: CC1). ***G–I***, In peripheral nervous system, MIF is expressed in DRG neurons (***G***, green: NF) and sciatic nerve axons (***H***, green: NF) but not the myelin sheath (***I***, green: myelin basic protein (MBP)). ***J***, After nerve injury (12 h post-injury), MIF is expressed by leukocytes, primarily macrophages (green, OX-42) at the epineurium-nerve interface (demarcated by arrows). In the DRG (*G*), MIF is also apparent in satellite cells (NF-negative cells cuffing neurons, demarcated by arrows). *A–J*: Scale bars = 20 μm. ***K***, ***L***, Specificity of anti-MIF labeling was confirmed in *Mif−/−* mouse spinal cord tissue. Despite high background in wild type C57BL/6 mouse tissue, positive labeling is discernible and shown here in dorsal horn cells, including neurons (arrowheads) (K). This labeling is absent in *Mif*−/− tissue (L). Scale bar for *K, L*=50 μm.

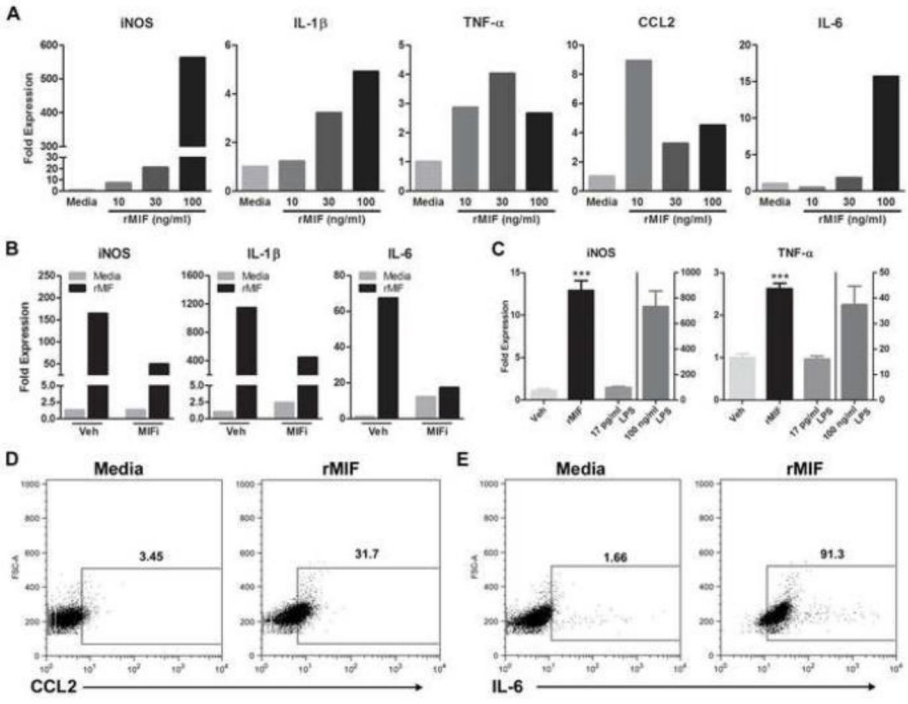

Figure 4.

MIF elicits inflammatory signaling in microglia. ***A***, Treatment of rat primary microglia with rMIF (10, 30 or 100 ng/ml) for 6 h increases iNOS, IL-1β, TNF-α, CCL2, and IL-6 mRNA expression. Data are normalized to an internal control gene (18s) then are expressed relative to mRNA changes elicited by media. Data are representative of three independent experiments. ***B***&***C***, Specificity of rMIF effects on microglia phenotype. ***B***, Co-application of MIF inhibitor (MIFi; 100 μM) with rMIF for 6 h reduces rMIF-induced cytokine gene expression. ***C***, rMIF effects on microglia phenotype are not due to endotoxin contamination - only trace amounts (17 pg/ml) of endotoxin were detected in rMIF. When treated with 17 pg/ml LPS for 6 h, BV-2 microglia did not increase expression of iNOS or TNF-α. Conversely, 6 h of stimulation with rMIF (100 ng/ml) or high concentrations of LPS (100 ng/ml) markedly induced expression of cytokines (***$p < 0.0001$ vs. Veh and 17 pg/ml LPS). ***D***&***E***, rMIF treatment of BV-2 microglia for 12h increases CCL2 and IL-6 protein. Representative contour plots show relative expression profiles for ***D***, CCL2 and ***E***, IL-6 in CD11b+ BV-2 microglia after 12 h of stimulation with media or rMIF (100 ng/ml). The mean percent of CCL2 or IL-6 expressing CD11b+ cells is indicated for each group. Dot plots are representative of two independent replicate experiments. Results are expressed as mean ± SEM.

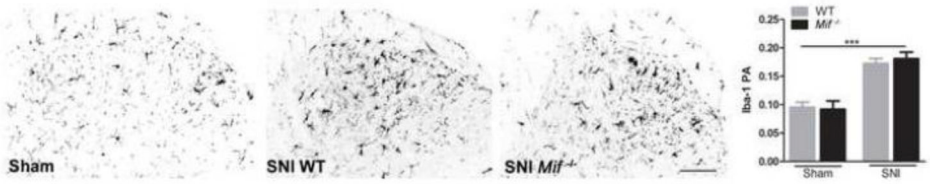

Figure 5.

Spinal cord dorsal horn microglial activation ipsilateral to nerve injury (SNI). Iba-1 immunoreactivity is increased by nerve injury compared to sham at 3 days (* vs. sham of same genotype). The microglial response to injury (or sham) does not differ between WT and *Mif* −/− mice. N=3 sham; N=5 SNI. PA: proportional area. Scale bar = 100 μm. Results are expressed as mean ± SEM. ****p*<0.0001

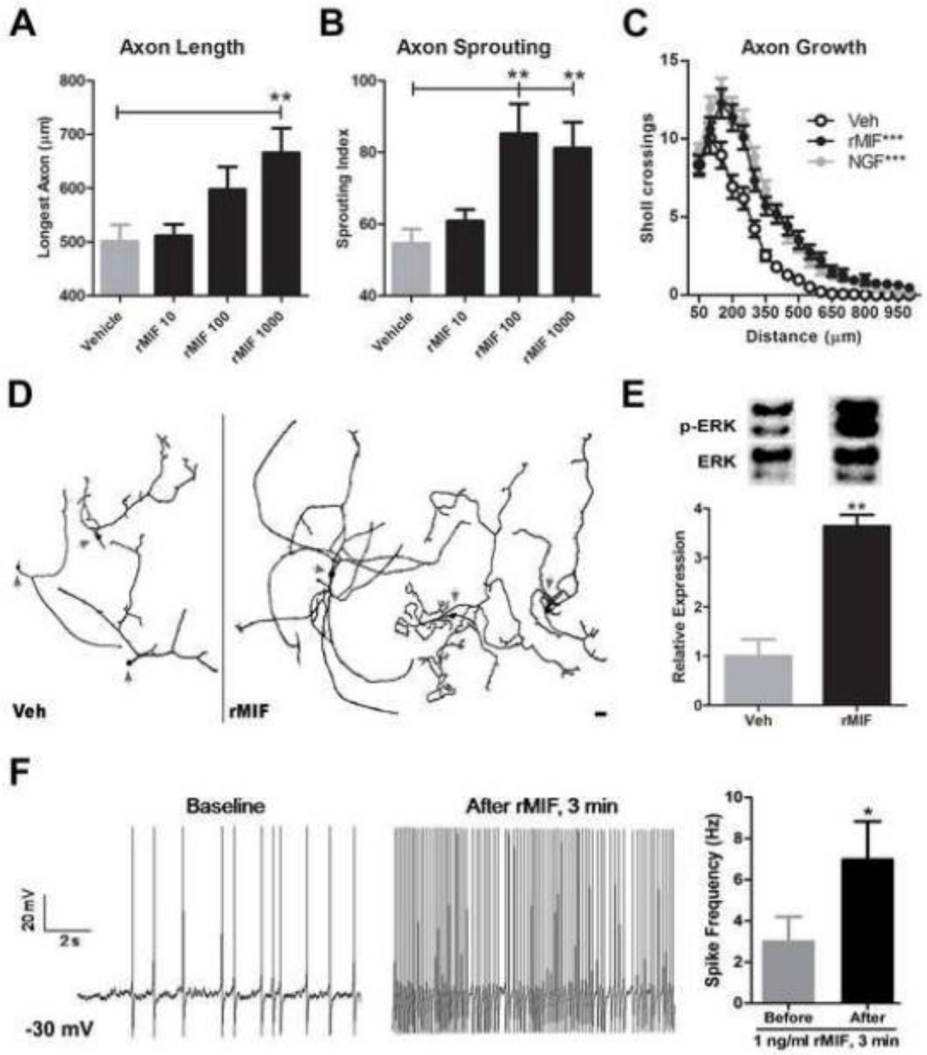

Figure 6.

rMIF increases structural and functional plasticity in sensory neurons. Twenty-four hours after plating, adult DRG neurons were treated with rMIF (10, 100, 1000 pg/ml). Forty eight hours later, the overall length and branching complexity of DRG axons was examined by Sholl analysis. ***A***, rMIF (1000 pg/ml) increased long-distance axon growth and ***B***, sprouting/branching complexity. ***C***, A composite view of axon length (distance) and sprouting shows that rMIF and NGF have nearly identical effects on promoting DRG axon growth (***: vs. Veh; $p>0.05$ rMIF vs. NGF.) ***D***, Representative DRG neurons (arrows delineate somata) treated with vehicle (Veh) or rMIF (1000 pg/ml) illustrate the neurotrophic effects of rMIF. Data in ***A–D*** obtained from n= 75–100 neurons per group (see Methods). Scale bar in D = 100μm. ***E***, ERK activation in DRG neurons after 10 min Veh or rMIF (1000 pg/ml) treatment. ***F***, MIF increases the excitability of small diameter DRG neurons. Current-clamp recordings from the same neuron showing the effects of exposure to rMIF (1 ng/ml). Mean neuron spike frequency measured after current clamp at −30 mV and after 3 min rMIF exposure (n=7 neurons). Results are expressed as mean ± SEM. Unless noted otherwise above, all statistical comparisons were made between rMIF vs. Veh treatments; *$p<0.05$; **$p<0.01$; ***$p<0.0001$.

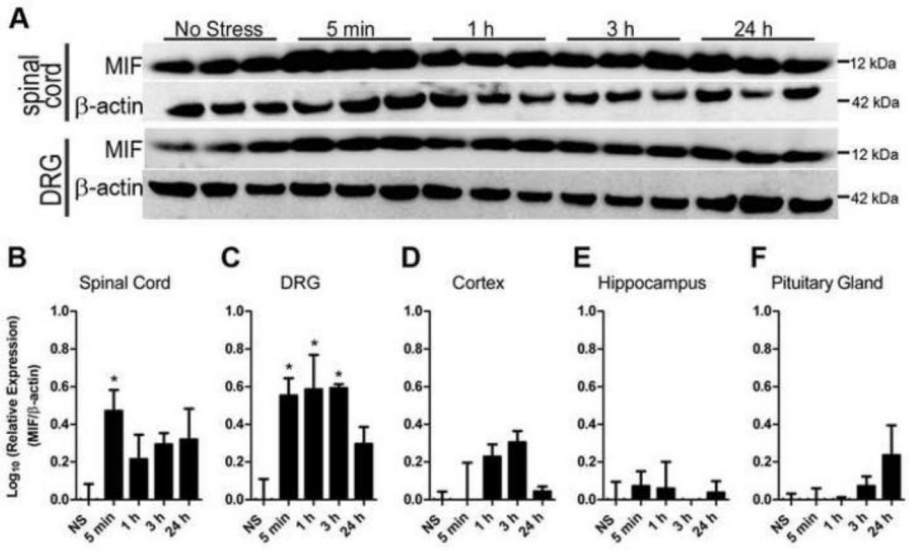

Figure 7.

Tissue MIF levels are increased by acute stress. ***A***, Western blot analysis of MIF in spinal cord and DRG after stress. ***B–F***, Quantitation of stress-induced MIF expression. Tissue MIF levels were normalized to β-actin and expressed relative to No Stress samples (NS) then log transformed to normalize distribution. Samples were collected 5 min or 1, 3 or 24 h after the onset of restraint stress or no stress. N=3 mice/per time point. Data expressed as mean ± SEM. *$p<0.05$

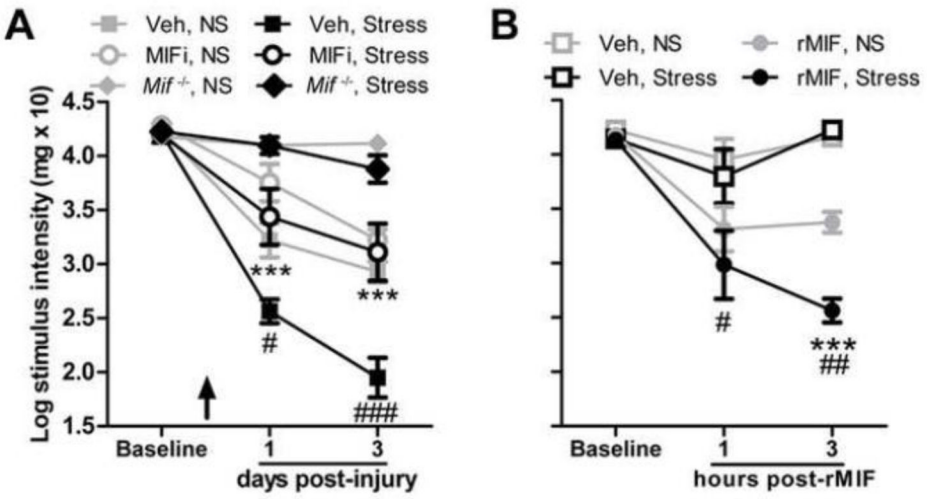

Figure 8.

MIF inhibition prevents stress-enhanced mechanical hypersensitivity. ***A***, A single systemic injection of MIFi prior to stress (demarcated by arrow) prevents stress-enhanced hypersensitivity caused by nerve injury. (#: Veh, No Stress (NS) vs. Veh, Stress; *: Veh, Stress vs. MIFi, Stress). Pain-like responses cannot be elicited by SNI nor are they enhanced by stress in *Mif*−/− mice. ***B***, Acute stress prior to i.pl. rMIF (1000 pg) increases mechanical hypersensitivity (* vs. rMIF, No Stress (NS); #: Veh, NS vs. rMIF, NS). y-axis values represent von Frey hair handle markings where 4.31=2 grams of force and 2.83=0.07 grams of force. N=5/group. Results are expressed as mean ± SEM. *#/*p*<0.05; ##/**p*<0.01; ###/***p*<0.0001